Fully self-consistent Hartree-Fock calculation of jellium slabs: Exact treatment of the exchange operator

Hongjun Luo and Wolfgang Hackbusch
Max-Planck-Institut für Mathematik in den Naturwissenschaften, Inselstr. 22-26, D-04103 Leipzig, Germany

Heinz-Jürgen Flad*
Institut für Informatik, Christian-Albrechts-Universität zu Kiel, Christian-Albrechts-Platz 4, D-24098 Kiel, Germany

Dietmar Kolb
Fachbereich Naturwissenschaften, Universität Kassel, Heinrich-Plett-Str. 40, D-34132 Kassel, Germany
(Received 15 October 2007; revised manuscript received 5 June 2008; published 31 July 2008)

We present Hartree-Fock surface energies, work functions, and dipole barriers for a Jellium slab model at different electron densities and slab widths. The fully self-consistent calculations take into account the nonlocal exchange coupling of the momentum parallel to the surface with the perpendicular component of the orbitals. Typical oscillations due to quantum-size effects have been observed. Our results provide lower and upper bounds for the Hartree-Fock surface energy and work function of the semi-infinite jellium model which can serve as benchmarks for previously reported variational calculations performed with different types of non-self-consistent orbitals. Furthermore we observed the expected characteristic band structures and electron densities, i.e., vanishing density of states at the Fermi energy and pronounced Friedel oscillations at jellium surfaces. In order to resolve the perpendicular components of the orbitals we have used a wavelet based interpolating scaling function basis.

DOI: 10.1103/PhysRevB.78.035136 PACS number(s): 73.20.At, 71.10.Ca, 31.15.xr, 02.70.Dh

I. INTRODUCTION

Quasi-two-dimensional many-electron systems such as graphite layers, thin films of metals, or semiconductor heterostructures are rewarding objects concerning their basic physical properties and possible applications in nanotechnology.[1,2] In order to deal with these systems from a computational point of view it is essential to take their quasi-two-dimensional character properly into account. Basically we have to deal with two-scale problems which can be handled using techniques from multiscale analysis. Recently wavelet based multiscale methods attracted considerable interest in solid-state physics[3–9] and quasi-two-dimensional systems might be an appropriate testing ground for the development of that kind of approach. Within our previous work, we have outlined a wavelet based Hartree-Fock (HF) method[10] especially adapted to the quasi-two-dimensional setting that can be further extended to incorporate electron correlations.[11,12]

Indispensable for method development are some kind of model problems which are simple enough to be solved with any desired accuracy and nonetheless contain the essential physics of more realistic systems. Paradigms for such problems are jellium surface and slab models. These are the simplest models for the study of electronic properties of metal surfaces and thin metallic films, cf. Ref. 13 for a review on this subject. Within these models only valence-band electrons are taken into account and contributions to the atomic charge density due to nuclei and core electrons have been replaced by a uniform background charge. Because of this rather crude approximation, at best qualitative agreement with physical properties of real metals can be expected. This has been already observed by Lang and Kohn[14,15] in their pioneering work on surface energies and work functions of metallic surfaces. Presently, the actual significance of jellium models is their role as a benchmark problem for density-functional theory (DFT), cf. Refs. 16–28. Because of the apparent simplicity of these models it is possible to perform fairly accurate calculations using many-particle wave functions. Following the early work of Sun and co-workers[29,30] using Jastrow-type correlation functions, and the more refined Fermi-hypernetted-chain (FHNC) calculations by Krotscheck and co-workers,[31,32] quantum Monte Carlo[33,34] (QMC) has been applied to jellium surfaces. The latter takes into account all kind of many-body correlations and should be considered as "exact" for jellium slabs except of the fixed-node approximation which means that the nodal domains are chosen with respect to a given approximate trial wave function. Therefore QMC calculations were intended as rigorous benchmarks for surface properties in order to judge the quality of approximate density functionals in the presence of a strong inhomogeneity of the electron density at the jellium surface. It turned out that there exist apparent discrepancies between QMC and results from DFT obtained for various types of density functionals and a DFT based random-phase approximation.[22,24,27] Presently, the controversy concerning these discrepancies has still not been fully settled, cf. Refs. 13, 35, and 36.

Within the present work, we focus on the HF method for jellium slabs. We expect some benchmarks for our more general approach, discussed in Ref. 10, which have been devised for inhomogeneous background charge densities as well. Amazingly there have been no fully self-consistent HF calculations for jellium surfaces or slabs reported in the literature. This is due to the nonlocal exchange operator present in the HF equations, which makes the perpendicular component

of the orbitals depending on the momentum parallel to the slab. However, numerous approximate HF calculations, following the pioneering work of Bardeen,[37] have been reported in the literature.[24,38–43] The variational HF calculations of Sahni and co-workers[44–46] rely on linear potential models which are explicitly solvable and provide reasonable trial wave functions which can be optimized with respect to the slope parameter for the HF energy functional. The slope parameter characterizes the slope of a linear effective potential which approximates among others the nonlinear Coulomb and exchange parts in the Fock operator. For a thorough discussion of the effective potential we refer to Sahni's monograph.[47] Since the HF bulk limit is well known, it is possible to obtain rigorous upper bounds for HF surface energies[39] and fairly accurate results for HF work functions.

II. HARTREE-FOCK EQUATIONS FOR A JELLIUM SLAB

We consider a neutral unpolarized jellium slab of finite width L and two large parallel surfaces Ω_+ and Ω_- each with area S. For technical reasons, periodic boundary conditions have been chosen in the parallel directions to the surfaces. Finally, the limit $S\to\infty$ has been taken. The closed-shell HF equations,[48,49] in atomic units, are given by

$$-\frac{1}{2}\Delta\psi_{n,\mathbf{k}_\parallel}(\mathbf{r}_\parallel,z)+\int_{-\infty}^{\infty}dz'\int_{\Omega}d^2r'_\parallel[\rho(z')-\rho_+(z')]\mathcal{V}(\mathbf{r}_\parallel-\mathbf{r}'_\parallel,z-z')\psi_{n,\mathbf{k}_\parallel}(\mathbf{r}_\parallel,z)-\sum_{n',\mathbf{k}'_\parallel}^{\text{occ}}\int_{-\infty}^{\infty}dz'\int_{\Omega}d^2r'_\parallel\psi_{n,\mathbf{k}_\parallel}(\mathbf{r}'_\parallel,z')\psi^*_{n',\mathbf{k}'_\parallel}(\mathbf{r}'_\parallel,z')$$
$$\times\mathcal{V}(\mathbf{r}_\parallel-\mathbf{r}'_\parallel,z-z')\psi_{n',\mathbf{k}'_\parallel}(\mathbf{r}_\parallel,z)=\epsilon_{n,\mathbf{k}_\parallel}\psi_{n,\mathbf{k}_\parallel}(\mathbf{r}_\parallel,z), \tag{2.1}$$

where $\mathbf{r}_\parallel$ and z denote the electron coordinates in a parallel section Ω of the slab and in the direction perpendicular to the surface. Because of periodic boundary conditions in the parallel directions, we require instead of the Coulomb potential a two-dimensional Ewald potential

$$\mathcal{V}(\mathbf{r}_\parallel,z)=\frac{2\pi}{S}\sum_{\mathbf{k}_\parallel\neq 0}\frac{1}{k_\parallel}e^{i\mathbf{k}_\parallel\cdot\mathbf{r}_\parallel-k_\parallel|z|}-\frac{2\pi}{S}|z|, \tag{2.2}$$

which is periodic in $\mathbf{r}_\parallel$. For simplicity we have taken a representation with summation in reciprocal space only, cf. Ref. 50 for further details. A positive background charge density

$$\rho_+(z)=\begin{cases}\rho_0, & |z|\le L/2\\ 0, & |z|>L/2\end{cases}, \tag{2.3}$$

which is constant inside the slab and drops abruptly at its surfaces, guarantees charge neutrality. Due to translational symmetry in the directions parallel to the surfaces, the HF orbitals are of the form

$$\psi_{n,\mathbf{k}_\parallel}(\mathbf{r}_\parallel,z)=\frac{1}{\sqrt{S}}\xi_{n,\mathbf{k}_\parallel}(z)e^{i\mathbf{k}_\parallel\cdot\mathbf{r}_\parallel},$$

with

$$\int_{-\infty}^{\infty}dz\xi^*_{n,\mathbf{k}_\parallel}(z)\xi_{n',\mathbf{k}_\parallel}(z)=\delta_{n,n'}, \tag{2.4}$$

where the perpendicular component ξ of the orbitals depends on the parallel momentum $\mathbf{k}_\parallel$. Furthermore, the electron density ρ depends only on the perpendicular coordinate z. In the limit $S\to\infty$, the slab becomes fully isotropic with respect to the parallel directions and therefore ξ depends only on the scalar momentum $k_\parallel$. The $\mathbf{k}_\parallel$ dependence of ξ is caused by couplings of momenta in the nonlocal exchange operator. Such kind of couplings are absent in one-particle models with purely local potentials, such as DFT where only a local exchange-correlation potential appears in the Kohn-Sham (KS) equation or the linear potential model mentioned previously. For this reason, previous work relied on orbitals which have been obtained from approximate HF models with purely local potentials. Based on the ansatz (2.4), the HF equations can be brought into a one-dimensional form

$$-\frac{1}{2}\frac{d^2}{dz^2}\xi_{n,\mathbf{k}_\parallel}(z)-2\pi\int_{-\infty}^{\infty}dz'[\rho(z')-\rho_+(z')]|z-z'|\xi_{n,\mathbf{k}_\parallel}(z)+\sum_{n'}^{\text{occ}}\int_{-\infty}^{\infty}dz'\xi_{n,\mathbf{k}_\parallel}(z')\xi^*_{n',\mathbf{k}_\parallel}(z')v_x^{(n')}(\mathbf{k}_\parallel,z-z')\xi_{n',\mathbf{k}_\parallel}(z)$$
$$=\left(\epsilon_{n,\mathbf{k}_\parallel}-\frac{1}{2}\mathbf{k}_\parallel^2\right)\xi_{n,\mathbf{k}_\parallel}(z), \tag{2.5}$$

with

$$v_x^{(n')}(\mathbf{k}_\parallel, z-z') = -\frac{2\pi}{S}\sum_{\mathbf{k}'_\parallel \neq \mathbf{k}_\parallel}^{\mathrm{occ}(n')} \frac{e^{-|\mathbf{k}'_\parallel - \mathbf{k}_\parallel||z-z'|}}{|\mathbf{k}'_\parallel - \mathbf{k}_\parallel|} + \frac{2\pi}{S}\sum_{\mathbf{k}'_\parallel}^{\mathrm{occ}(n')} |z-z'|\delta_{\mathbf{k}'_\parallel,\mathbf{k}_\parallel}, \tag{2.6}$$

where the representation (2.2) of the Ewald potential has been used to get rid of the dependence on parallel coordinates $\mathbf{r}_\parallel$. By definition ρ and ρ_+ are even functions of z, therefore the second term on the left side of Eq. (2.5) vanishes for $z \to \pm\infty$. An expression, similar to Eq. (2.6), for the exchange term has been already obtained by Bardeen.[37] Due to a finite width of the slabs, the quantum number n associated with the perpendicular direction remains discrete. This so-called size quantization gives rise to certain finite width effects[51,52] which will be further discussed below. In Fig. 1, a schematic plot shows the orbital energies $\epsilon_{n,k_\parallel}$ in the limit $S \to \infty$, which depend on the continuous quantum number $k_\parallel$ and the discrete quantum number n associated with the parallel and the perpendicular directions, respectively. To each quantum number n a Fermi momentum, denoted by $k_F^{(n)}$, has been assigned. In the limit $S \to \infty$, the electron density becomes

$$\rho(z) = \lim_{s\to\infty}\frac{2}{S}\sum_{n,\mathbf{k}_\parallel}^{\mathrm{occ}} \xi^*_{n,\mathbf{k}_\parallel}(z)\xi_{n,\mathbf{k}_\parallel}(z) = \frac{1}{\pi}\sum_n^{\mathrm{occ}} \int_{k_\parallel \le k_F^{(n)}} k_\parallel dk_\parallel \xi^*_{n,k_\parallel}(z)\xi_{n,k_\parallel}(z), \tag{2.7}$$

where we have replaced the sum over $\mathbf{k}_\parallel$ by the corresponding integral in the large S limit

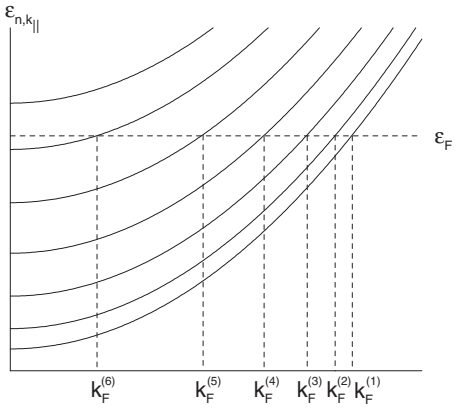

FIG. 1. Schematic plot of orbital energies $\epsilon_{n,k_\parallel}$ and Fermi momenta $k_F^{(n)}$.

$$\frac{1}{S}\sum_{\mathbf{k}_\parallel} \to \frac{1}{(2\pi)^2}\int d^2k_\parallel. \tag{2.8}$$

The Fermi energy ϵ_F is determined by the charge neutrality condition

$$\sum_n (k_F^{(n)})^2 = 2\pi\sigma_0, \tag{2.9}$$

where $\sigma_0 = \rho_0 L$ is the surface background charge density.

The third term on the left-hand side of Eq. (2.5) represents the nonlocal exchange operator and constitutes the most difficult part from a computational point of view. In the limit $S \to \infty$ it becomes

$$-\frac{1}{2\pi}\sum_{n'}\int_{|\mathbf{k}'_\parallel|\le k_F^{(n')}} d^2k'_\parallel \int_{-\infty}^{\infty} dz' \xi_{n,k_\parallel}(z')\xi^*_{n',k'_\parallel}(z')\xi_{n',k'_\parallel}(z)\frac{e^{-|\mathbf{k}_\parallel - \mathbf{k}'_\parallel||z-z'|}}{|\mathbf{k}_\parallel - \mathbf{k}'_\parallel|} = -\sum_{n'}\int_{k'_\parallel \le k_F^{(n')}} dk'_\parallel \int_{-\infty}^{\infty} dz' \xi_{n,k_\parallel}(z')\xi^*_{n',k'_\parallel}(z')\xi_{n',k'_\parallel}(z) I(k_\parallel, k'_\parallel, |z-z'|), \tag{2.10}$$

where we have introduced the function

$$I(k_\parallel, k'_\parallel, |z-z'|) = \frac{1}{2\pi}\int_0^{2\pi} d\theta' \frac{k'_\parallel \exp(-|z-z'|\sqrt{k_\parallel^2 + k_\parallel'^2 - 2k_\parallel k'_\parallel \cos\theta'})}{\sqrt{k_\parallel^2 + k_\parallel'^2 - 2k_\parallel k'_\parallel \cos\theta'}}, \tag{2.11}$$

which can be partly precomputed and stored prior to the actual HF calculation. A detailed discussion of the numerical treatment of the function $I(k_\parallel, k'_\parallel, |z-z'|)$ has been given in Appendix A.

The HF energy per unit surface area of the slab is given by

$$\lim_{s\to\infty}\frac{E_{\mathrm{slab}}}{2S}=\frac{1}{4\pi}\sum_{n}^{\mathrm{occ}}\int_{k_\parallel<k_F^{(n)}}k_\parallel dk_\parallel\int_{-\infty}^{\infty}dz\left\{\left[\frac{d}{dz}\xi_{n,k_\parallel}(z)\right]^2+k_\parallel^2\xi_{n,k_\parallel}^2(z)\right\}-\frac{\pi}{2}\int_{-\infty}^{\infty}dz\int_{-\infty}^{\infty}dz'[\rho(z)-\rho_+(z)]|z-z'|[\rho(z')-\rho_+(z')]$$
$$-\frac{1}{4\pi}\sum_{n,n'}^{\mathrm{occ}}\int_{k_\parallel\le k_F^{(n)}}k_\parallel dk_\parallel\int_{k_\parallel'\le k_F^{(n')}}dk_\parallel'\int_{-\infty}^{\infty}dz\int_{-\infty}^{\infty}dz'\,\xi_{n,k_\parallel}^*(z)\xi_{n,k_\parallel}(z')\xi_{n',k_\parallel'}^*(z')\xi_{n',k_\parallel'}(z)I(k_\parallel,k_\parallel',|z-z'|),\tag{2.12}$$

which together with the corresponding expression for bulk jellium,[48]

$$\frac{E_{\mathrm{bulk}}}{2S}=\left(\frac{1.104\ 95\ \ \mathrm{a.u.}}{r_s^2}-\frac{0.458\ 165\ \ \mathrm{a.u.}}{r_s}\right)\frac{\rho_0 L}{2},\tag{2.13}$$

can be used to calculate the HF surface energy of a jellium slab

$$E_s=\lim_{s\to\infty}\frac{E_{\mathrm{slab}}-E_{\mathrm{bulk}}}{2S}.\tag{2.14}$$

Here the dimensionless parameter r_s refers to the Wigner-Seitz radius

$$r_s=\left(\frac{3}{4\pi\rho}\right)^{1/3}/a_B,\tag{2.15}$$

where a_B denotes the Bohr radius.

Another important property is the work function W, which is defined as the minimum energy required to detach an electron from the jellium slab. The electrostatic potential

$$v(z)=-2\pi\int_{-\infty}^{\infty}dz'[\rho(z')-\rho_+(z')]|z-z'|\tag{2.16}$$

vanishes in the limit $z\to\pm\infty$ due to charge neutrality and inversion symmetry of the densities ρ and ρ_+. According to Koopman's theorem, the HF work function therefore corresponds to minus the Fermi energy, i.e.,

$$W=-\epsilon_F.\tag{2.17}$$

It should be mentioned that relaxation effects can be neglected for an infinitely extended slab and Eq. (2.17) becomes an exact expression for the work function on the HF and local-density approximation (LDA) level of theory, cf. Refs. 53 and 54. This however requires a fully self-consistent solution of the HF or KS equations which hitherto has not been accomplished for the HF method. An alternative approach, which is less sensitive with respect to an error of the wave function, is the displaced-profile change-in-self-consistent-field (DPΔSCF) method.[54,55] Therefore, the DPΔSCF method is particularly accurate for variational calculations.[55] It should be mentioned that both approaches become equivalent in the SCF limit.

According to Lang and Kohn,[15] an alternative expression for the work function $W=\Delta\Phi-\bar{\mu}$ of the semi-infinite jellium model, which is especially appropriate for DFT, can be given in terms of the surface dipole barrier $\Delta\Phi$ and the bulk chemical potential of the electrons $\bar{\mu}$ relative to the mean electrostatic potential in the interior of the metal. Because of its significance in the literature we have calculated the dipole barrier for jellium slabs,

$$\Delta\Phi=2\pi\int_{-\infty}^{\infty}dz[\rho(z)-\rho_+(z)]|z|,\tag{2.18}$$

as the difference of the electrostatic potentials at infinity and at the center of the slab.

III. SELF-CONSISTENT-FIELD HARTREE-FOCK CALCULATIONS

The discretization of the perpendicular components $\xi_{n,k_\parallel}$ of the orbitals requires a very flexible basis set which is capable to approximate the steep decay at the jellium surface and the harmonic oscillations deep inside the slab with similar efficiency. We have chosen an interpolating scaling function basis of high order from multiresolution analysis. For further details concerning the Galerkin discretization of the HF equations and the self-consistent-field (SCF) iteration scheme we refer to Appendix B.

A good initial guess for the orbitals is mandatory for the self-consistent solution of the HF equations for jellium slabs. In our HF calculations, we prepared these initial orbitals via linear potential and subsequent fully self-consistent LDA calculations. These calculations require a comparatively small computational effort, because for KS orbitals the perpendicular components ξ_n^{LDA} do not depend on the momentum parallel to the slab. A further merit of this approach is that a direct comparison can be made between quantum-size effects at finite slab widths for LDA and HF calculations. Our results presented below demonstrate that HF exhibits more pronounced quantum-size effects than LDA.

A. Preparatory self-consistent-field LDA calculations

For computational simplicity and in order to enable a direct comparison of our results with previous work for the semi-infinite jellium model, we have chosen Wigner's local approximation for the exchange-correlation potential[56] in the corrected form used by Lang and Kohn.[15] A straightforward SCF iteration scheme does not converge, which has been already noted by Lang and Kohn.[14] A simple but rather inefficient approach introduces a mixing parameter $0<p_{\mathrm{mix}}\le 1$ into the updating scheme

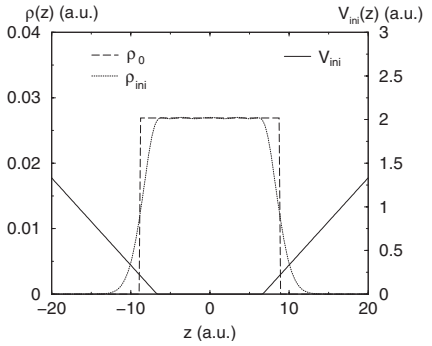

FIG. 2. Linear potential model and the initial guess for the electron density.

$$v^{\mathrm{LDA}}(z) := (1 - p_{\mathrm{mix}})v^{\mathrm{LDA}}_{\mathrm{old}}(z) + p_{\mathrm{mix}}v^{\mathrm{LDA}}_{\mathrm{new}}(z) \qquad (3.1)$$

for the nonlinear exchange-correlation potential. In our calculations, p_{mix} has to be chosen rather small, i.e., 10^{-2}–10^{-3}, in order to guarantee convergence of the SCF iterations. The initial guess for the SCF iteration has been obtained from a linear potential model,[44–46] which is depicted schematically in Fig. 2. We have adjusted the parameters of the linear potential model in order to reproduce the correct density inside the slab. Calculations have been performed for various slab widths and three different bulk electron densities, i.e., r_s=2, 4, and 6, corresponding to the high, medium, and low density regime, respectively.

In Fig. 3, we have plotted self-consistent LDA surface energies, dipole barriers, and work functions versus slab width for different electron densities. Such kind of calculations have been already appeared in the literature, cf. Ref. 51

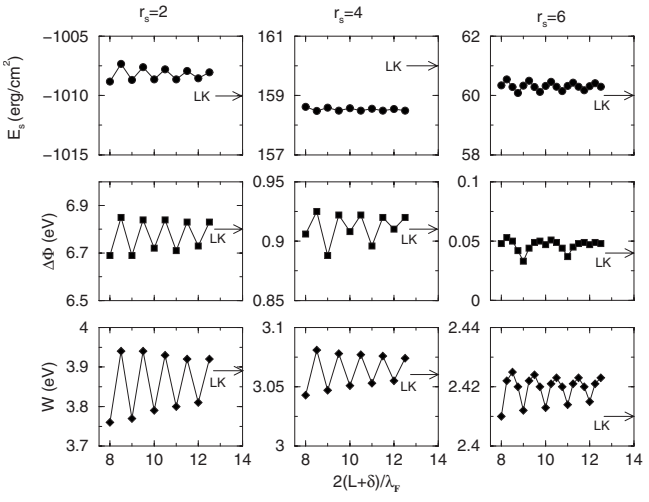

FIG. 3. Self-consistent LDA surface energy E_s (erg/cm^2), dipole barrier $\Delta\Phi$ (eV), and work function W (eV) for various slab widths L and electron densities r_s=2, 4, and 6. The quantities are plotted versus $2(L+\delta)/\lambda_F$ which approaches integer values at the touching point of a formerly unoccupied band with the Fermi surface. The shift parameter δ has been adjusted to 0.327, −1.244, and −2.947 bohrs for r_s=2, 4, and 6, respectively. Arrows (LK) indicate the results of Lang and Kohn (Refs. 14 and 15) for the semi-infinite jellium model.

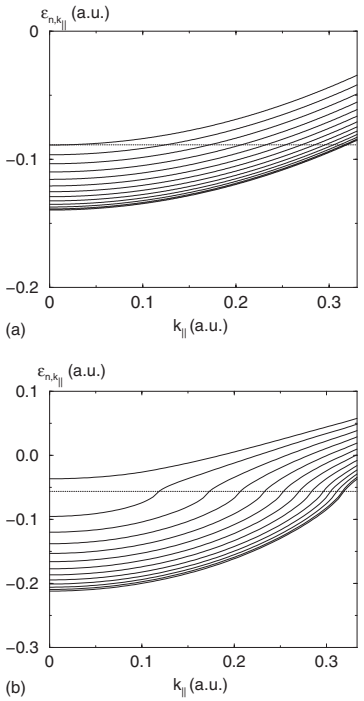

FIG. 4. Orbital energies $\epsilon_{n,k_\parallel}$ obtained from (a) LDA and (b) HF calculations for a jellium slab with r_s=6 and $2(L+\delta)/\lambda_F$=12.

for the work function and Ref. 24 for the surface energy. The typical oscillatory behavior of these quantities is due to the fact that with increasing slab width, the unoccupied bands become lower in energy and at certain slab widths the respective lowest unoccupied band touches and finally crosses the Fermi surface. These touching points appear with an expected periodicity $\lambda_F/2$ with respect to the effective slab width $L+\delta$, where $\lambda_F := 2\pi/k_F$ denotes the Fermi wavelength of the bulk. To take into account the leakage of electron density at the jellium surface, the slab width has to be corrected by a shift parameter δ. The underlying mechanism for this periodicity has already been discussed by Schulte[51] for self-consistent LDA calculations of jellium slabs and more recently by Pitarke and Eguiluz[24] within the *infinite barrier model* where a rigorous notion can be given to the parameter δ. The motivation for the latter work was to derive an efficient extrapolation scheme in order to derive results for the semi-infinite jellium model from calculations with finite slab widths. Within our calculations we have adjusted the parameter δ for each electron density in such a manner that integer values of the function $2(L+\delta)/\lambda_F$ approximately correspond to touching points in the band structure. This situation is shown in Fig. 4(a). It turned out that in order to adjust this parameter with good accuracy it was sufficient to consider only a single touching point at each electron density. For r_s=2, 4 and 6, the parameter δ assumes values of 0.327, –1.244, and –2.947 bohrs, respectively. The change of sign can be already inferred from Fig. 8 of Ref. 51.

It can be seen from Fig. 3 that our results for the surface energy E_s have been already converged with respect to the slab width within an accuracy of 1 erg/cm^2 and were found to be in excellent agreement with the values reported by Lang and Kohn.[14] Variational LDA calculations based on the

linear potential model[44] provide fairly accurate upper bounds for these surface energies. We did not attempt a further extrapolation of our results along the lines of Ref. 24, because we expected that at such small energy differences the periodic behavior is already affected by superpositions with discretization errors. Similarly our results for the work function W and dipole barrier $\Delta\Phi$ have already reached a high degree of convergence and were found to be in very good agreement with the results of Lang and Kohn.[15] The DPΔSCF work functions of Ref. 55 as well are in good agreement with these results and demonstrate the enhanced accuracy of this approach for variational calculations.

B. Self-consistent Hartree-Fock calculations

Unlike LDA, the HF-SCF iterations have to be performed for every $k_{\|}$ point separately and the Fock matrix must be updated after every such step. We refer to Appendix B for further details. Starting with an initial guess generated from an LDA calculation, the convergence of HF-SCF iterations turned out to be very stable. In the high-density regime (r_s=2), the surface energy converges monotonously even without using a damping parameter. For the other two densities (r_s=4 and 6), a damping parameter p_{mix}=0.5, for the nonlinear part of the Fock operator, cf. Eq. (3.1), assures convergence. Typically, fully converged results require 20 up to 100 iterations, depending on the slab width. Close to touching points in the LDA band structure, more iterations were needed than for slab widths in between.

The HF calculations have been performed for the same electron densities and slab widths as the LDA calculations discussed in Sec. III A. Peaks of quantum oscillations can be expected at approximately the same slab widths as for LDA. Since HF calculations are considerably more expensive we did not try to locate the precise position of the peaks with respect to the slab width. An exception was r_s=6, where the HF oscillation pattern at small slab widths turned out to be rather irregular. Therefore we have refined our grid in order to recover the slightly shifted maxima. Concerning the band structure, the situation for HF is actually qualitatively different from LDA, as can be seen by a comparison of the corresponding band structures shown in Figs. 4(a) and 4(b). Close to the Fermi surface, the slope of the partially occupied HF bands becomes very steep. Actually it is well known for bulk jellium that the bands should be perpendicular to the Fermi surface, which leads in HF to the vanishing of the density of states (DOS) at the Fermi energy shown in Fig. 5. Because of a finite mesh size for the discretization of $k_{\|}$, we cannot fully reproduce the vanishing DOS. Instead we observed a valley of the HF-DOS at the Fermi energy which is quite different from the monotonously increasing LDA-DOS also shown in the figure. It has been pointed out by Monkhorst[57] that the vanishing DOS at the Fermi energy for HF holds true in general for extended periodic system in three or lower dimensions. The steps in the DOS are typical quantum-size effects for finite slab width and have been discussed, e.g., in Ref. 52 for an independent-particle model. Due to this peculiar feature of HF band structures there are no touching points of lowest unoccupied bands with the Fermi surface anymore. Instead an abrupt jump below the Fermi surface occurs once the unoccupied band comes sufficiently close to it.

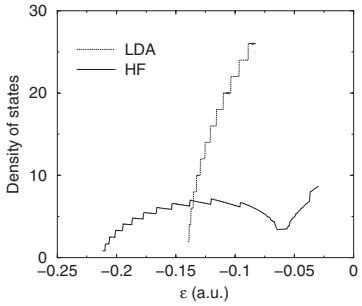

FIG. 5. HF and LDA-DOS for a jellium slab with r_s=6 and $2(L+\delta)/\lambda_F$=12.

Our results for the surface energy, depicted in Fig. 6, show the typical quantum oscillations with respect to the slab width. We have listed the values at slab widths roughly corresponding to maxima and minima of the surface energy in Table I. Compared with LDA, the HF oscillations turned out to be much stronger, as reference points serve the variational surface energies of Sahni and Ma[39] and of Pitarke and Eguiluz[24] for the semi-infinite jellium model. These authors used a HF energy functional but the orbitals have not been obtained from self-consistent calculations. Instead Sahni and Ma took orbitals from the linear potential model, whereas Pitarke and Eguiluz used exchange-only and Perdew-Zunger parametrized LDA orbitals obtained as self-consistent solutions of the corresponding KS equations. Their results represent upper bounds to the actual HF surface energies which is actually reflected by our calculations. It can be seen from

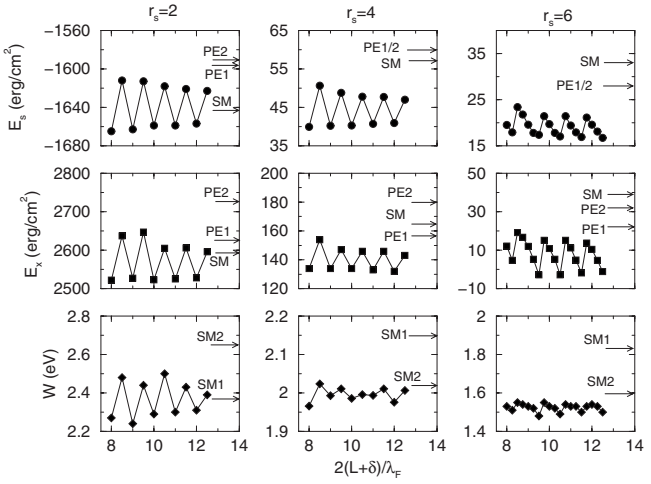

FIG. 6. Self-consistent HF surface energy E_s (erg/cm^2), exchange contribution to the surface energy E_x (erg/cm^2), and work function W (eV) for various slab widths L and electron densities r_s=2, 4, and 6. The quantities are plotted versus $2(L+\delta)/\lambda_F$ with LDA shift parameters δ. Arrows (SM) indicate the variational surface energies of Sahni and Ma (Ref. 39) and (SM1) and (SM2) indicate their work functions based on Koopman's theorem and DPΔSCF, respectively. Furthermore the arrows (PE1) and (PE2) indicate the exchange surface energies of Pitarke and Eguiluz (Ref. 24) obtained with LDA and exchange-only orbitals, respectively.

TABLE I. Self-consistent HF surface energy E_s (erg/cm^2), dipole barrier $\Delta\phi$ (eV), and work function W (eV) for various slab widths L and electron densities r_s=2, 4, and 6. The slab widths, given via $2(L+\delta)/\lambda_F$, roughly correspond to maxima and minima of the quantum oscillations. Lower and upper bounds of these quantities for the semi-infinite jellium model are indicated by ⌊ ⌋ and ⌈ ⌉, respectively. Kinetic E_k, electrostatic $E_{\rm es}$, and exchange E_x contributions (erg/cm^2) to the surface energy are listed separately. Results of Sahni and Ma (Ref. 39) as well as of Pitarke and Eguiluz (Ref. 24) from non-self-consistent HF calculations with various types of orbitals for the semi-infinite jellium model are listed for comparison.

$2(L+\delta)/\lambda_F$	E_k	E_{es}	E_x	E_s	$\Delta\Phi$	W
r_s=2, δ=0.327 bohrs						
8.0	−5456	1268	2522	−1665	6.76	2.27
8.5	−5571	1323	2637	−1612	6.94	2.48
9.0	−5465	1275	2527	−1663	6.74	2.24
9.5	−5560	1335	2647	−1613	6.96	2.44
10.0	−5454	1272	2523	−1659	6.79	2.29
10.5	−5524	1301	2605	−1618	6.90	2.50
11.0	−5458	1274	2525	−1659	6.76	2.30
11.5	−5537	1310	2606	−1621	6.90	2.43
12.0	−5462	1276	2528	⌊−1657⌋	⌊6.79⌋	⌊2.31⌋
12.5	−5522	1304	2596	⌈−1623⌉	⌈6.90⌉	⌈2.39⌉
Sahni-Ma	−5650	1414	2593	−1643	6.58	2.36[a],2.65[b]
Pitarke-Eguiluz[c]	−5495	1276	2624	−1595		
Pitarke-Eguiluz[d]	−5707	1390	2726	−1591		
r_s=4, δ=−1.244 bohrs						
8.0	−143	48	134	40	1.11	1.97
8.5	−152	49	154	51	1.14	2.02
9.0	−142	49	134	40	1.08	1.99
9.5	−147	49	147	49	1.09	2.01
10.0	−142	48	134	40	1.08	1.99
10.5	−147	49	146	48	1.12	2.00
11.0	−141	49	133	41	1.07	1.99
11.5	−147	49	146	48	1.09	2.01
12.0	−140	49	132	⌊41⌋	⌊1.07⌋	⌊1.98⌋
12.5	−145	49	143	⌈47⌉	⌈1.08⌉	⌈2.01⌉
Sahni-Ma	−150	43	164	57	1.12	2.15[a],2.02[b]
Pitarke-Eguiluz[c]	−139	42	157	60		
Pitarke-Eguiluz[d]	−169	49	180	60		
r_s=6, δ=−2.947 bohrs						
8.25	−1	14	5	18	0.29	1.51
8.5	−8	12	19	23	0.28	1.55
9.5	4	17	−3	17	0.15	1.48
9.75	−6	13	15	21	0.25	1.55
10.5	4	16	−3	17	⌈0.31⌉	1.49
10.75	−6	13	15	21	0.24	1.54
11.5	3	16	−2	17	⌊0.16⌋	1.50
11.75	−5	13	14	⌈21⌉	0.27	⌈1.53⌉
12.5	2	16	−1	⌊17⌋	0.29	⌊1.50⌋
Sahni-Ma	−14	8	39	33	0.45	1.83[a], 1.60[b]
Pitarke-Eguiluz[c]	−3	9	22	28		
Pitarke-Eguiluz[d]	−13	9	32	28		

[a]Koopman's theorem.
[b]DPΔSCF.
[c]LDA orbitals.
[d]exchange-only orbitals.

Table I that the surface energies from exchange-only and LDA orbitals are almost identical, however the individual contributions, to be discussed below, may differ considerably.

We refrain from extrapolating our results to the semi-infinite limit according to the scheme proposed by Pitarke and Eguiluz.[24] For sensible slab widths with $2(L+\delta)/\lambda_F$ between 8 and 13, the amplitudes of oscillations are already sufficiently small to provide meaningful estimates of the surface energy for the semi-infinite case as well. The convergence of the amplitudes, however, is rather slow and it has been already remarked in Sec. III A that our discretization error which is around 1 erg/cm^2 might depend on the slab widths in a sensible manner. Therefore it seems to be dubious to extrapolate the surface energies to the semi-infinite limit. Instead we have listed our results for different slab widths in Table I and provide only upper and lower bounds for the semi-infinite jellium model.

At high electron density ($r_s=2$) our surface energies oscillate around the variational result of Sahni and Ma[39] where the upper bound is approx. 30 erg/cm^2 lower than the values obtained by Pitarke and Eguiluz.[24] Our upper bound for the quantum oscillations at intermediate electron density, i.e., $r_s=4$, is approx. 10 erg/cm^2 lower than Sahni and Ma's variational surface energy which again is only slightly smaller than the value of Pitarke and Eguiluz. The latter obtained a lower surface energy at low electron density, i.e., $r_s=6$, compared with Sahni and Ma, which is approx. 7 erg/cm^2 higher than our upper bound. Despite of the small energy differences involved these results represent a fairly good agreement between the variational estimates and our fully self-consistent HF results at large slab widths. Concerning the exchange contribution to the surface energy it can be seen from Fig. 6 that the corresponding quantum oscillations are twice as large as for the total surface energy. Altogether the best agreement with variational calculations has been achieved for LDA orbitals. Our upper bounds for the quantum oscillations match very well with the values reported by Pitarke and Eguiluz.

Another important property we have studied is the work function. According to the discussion at the end of Sec. II, we have used Koopman's theorem to calculate the work function of jellium slabs. It can be seen from Fig. 6 that the quantum oscillations decrease with decreasing electron density with amplitudes, for $r_s=4$ and 6, well below 0.1 eV at large slab widths. In the variational but non-self-consistent calculations of Sahni and Ma,[39] the work function can be only computed approximately. Two different approximation methods have been discussed in their paper. Besides results based on Koopman's theorem, the DPΔSCF method has been considered, cf. our discussion at the end of Sec. II. The latter is supposed to be particularly accurate for the variational approach of Sahni and Ma.[54,55] By comparison, these two methods show significant differences of order 10%. For $r_s=2$ our results oscillate around their value based on Koopman's theorem whereas for $r_s=4$ and 6, the DPΔSCF value agrees very well with our calculations. An important contribution to the work function comes from the dipole barrier $\Delta\phi$, which has been also listed in Table I. The quantum oscillations for the dipole barrier are not that regular, which

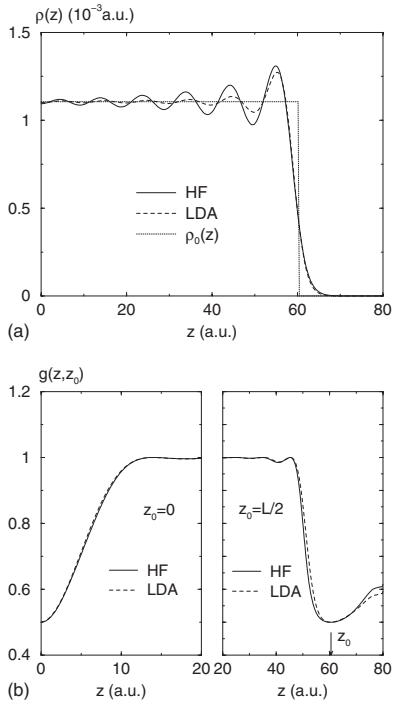

FIG. 7. Charge density and pair distribution function for a jellium slab with $r_s=6$ and $2(L+\delta)/\lambda_F=12$.

has been already observed for our LDA calculations. Nevertheless we can provide reasonable lower and upper bounds for the semi-infinite case. These bounds can be compared with the corresponding values of Sahni and Ma.[39] For $r_s=2$, their value is approx. 0.2 eV below our lower bound. An almost perfect agreement has been observed for $r_s=4$, whereas for $r_s=6$, Sahni and Ma's value is approx. 0.15 eV above our upper bound.

In spite of the nice overall agreement between our fully self-consistent HF results and the variational calculations of Sahni and Ma[39] as well as of Pitarke and Eguiluz[24] using different types of approximate orbitals, it is interesting to look for possible differences in the electron density and pair distribution function

$$g(z,z') = \frac{\langle \Phi_{\mathrm{HF}} \left| \sum_{i\neq j} \delta(\mathbf{r}-\mathbf{r}_i)\delta(\mathbf{r}'-\mathbf{r}_j) \right| \Phi_{\mathrm{HF}} \rangle|_{\mathbf{r}_\parallel=\mathbf{r}'_\parallel}}{\rho(z)\rho(z')}. \tag{3.2}$$

In Figs. 7(a) and 7(b) we compare the electron density and pair distribution function obtained from HF and LDA orbitals. Within DFT, it does not really make sense to consider a pair distribution function from KS orbitals, since they are only supposed to represent the electron density. However, the variational approach takes them as approximations to HF orbitals which represent via the corresponding Slater determinant an approximation to the full many-body wave function. It can be seen in Fig. 7(a) that the Friedel oscillations in the electron density near the surface of the slab are much stronger for HF, compared to LDA, and extent much farther into the slab. In the immediate neighborhood of the jellium surface, however, both electron densities agree fairly well.

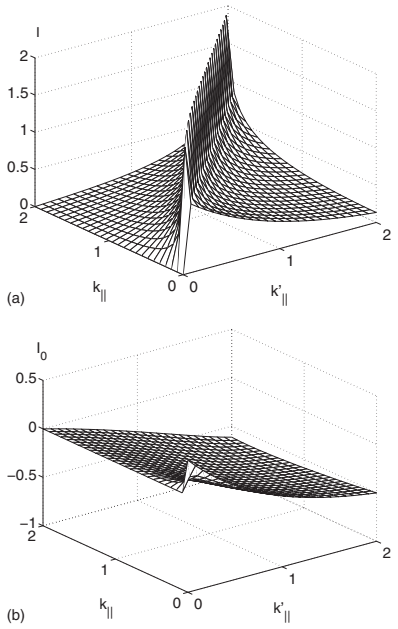

FIG. 8. Plots of the functions (a) $I(k_\parallel,k'_\parallel,1)$ and (b) $I_0(k_\parallel,k'_\parallel,1)$.

Concerning the pair distribution function we have considered two different situations. In the left part of Fig. 7(b), a reference electron was fixed at the center of the slab. As might be expected, the HF and LDA pair distribution functions are almost indistinguishable inside the slab. In contrast to this, marked differences can be seen if a reference electron is placed at the surface of the slab which is depicted on the right part of Fig. 7(b).

IV. CONCLUSIONS

We have performed fully self-consistent HF calculations for a Jellium slab model which take into account the coupling between the momentum parallel to the surface with the perpendicular component of the orbitals caused by the nonlocal nature of HF exchange. The HF band structure shows the characteristic vanishing DOS at the Fermi energy and the electron densities have enhanced Friedel oscillations near the jellium surface compared to LDA. With varying slab width, we observed the typical oscillations of the HF surface energy and work function due to quantum-size effects in the direction perpendicular to the surface. Compared to LDA, the HF method exhibits significantly stronger quantum oscillations. For large slab widths however, these oscillations are already sufficiently small in order to extract useful lower and upper bounds for the HF surface energy and work function of the semi-infinite jellium model. Our results serve as benchmarks for previously reported variational calculations[24,39] performed with different types of non-self-consistent orbitals. At medium and low electron densities our upper bounds of the HF surface energy are considerably lower than the upper bounds of Refs. 24 and 39. Furthermore we observed fairly good agreement between the approximate work functions of Sahni and Ma[39] and our fully self-consistent HF calculations using Koopman's theorem.

ACKNOWLEDGMENTS

This work was supported by the Deutsche Forschungsgemeinschaft Contract No. SPP 1095. The authors H.L. and D.K. gratefully acknowledge J. Dobson (Brisbane) for helpful discussions.

APPENDIX A: COMPUTATION OF THE FUNCTION $I(k_\parallel,k'_\parallel,|z-z'|)$

The function $I(k_\parallel,k'_\parallel,|z-z'|)$, cf. Equation (2.11), diverges logarithmically along the diagonal $k_\parallel=k'_\parallel$, cf. Fig. 8(a). Although this is a rather weak type of singularity, it has to be treated carefully when computing the exchange operator. In order to separate the divergent part, we split the function into two terms

$$I(k_\parallel,k'_\parallel,|z-z'|)=I_0(k_\parallel,k'_\parallel,|z-z'|)+I_1(k_\parallel,k'_\parallel), \tag{A1}$$

where the first function,

$$I_0(k_\parallel,k'_\parallel,|z-z'|)=\frac{1}{\pi}\int_0^\pi d\theta' \frac{k'_\parallel(\exp(-|z-z'|\sqrt{k_\parallel^2+k_\parallel'^2-2k_\parallel k'_\parallel\ \cos\ \theta'})-\cos\ (\theta'/2))}{\sqrt{k_\parallel^2+k_\parallel'^2-2k_\parallel k'_\parallel\ \cos\ \theta'}}, \tag{A2}$$

is well behaved except of a conical point at $\mathbf{k}_\parallel=\mathbf{k}'_\parallel=0$, cf. Fig. 8(b). The divergent part has been separated into the function $I_1(k_\parallel,k'_\parallel)$ which can be evaluated analytically:

$$I_1(k_\parallel,k'_\parallel)=\frac{1}{\pi}\int_0^\pi d\theta' \frac{k'_\parallel\ \cos\ (\theta'/2)}{\sqrt{k_\parallel^2+k_\parallel'^2-2k_\parallel k'_\parallel\ \cos\ \theta'}}$$
$$=\frac{1}{\pi}\frac{\sqrt{k'_\parallel}}{\sqrt{k_\parallel}}\ln\frac{\sqrt{k_\parallel}+\sqrt{k'_\parallel}}{|\sqrt{k_\parallel}-\sqrt{k'_\parallel}|}. \tag{A3}$$

For every discrete quantum number n, the functions $\xi_{n,k_\parallel}$ have been computed with respect to the parameter $k_\parallel$ on a regular mesh for the interval $[0,\kappa]$ with $k_F^{(n)}\leq\kappa$. In order to compute the exchange integrals (2.10), we consider piecewise constant approximations of the functions

$$\xi_{n,k_\parallel}(z)\approx\sum_i \xi_{n,k_i}(z)h_i(k_\parallel) \tag{A4}$$

with respect to the parameter $k_\parallel$, where h_i denotes the characteristic function on the ith subinterval $[k_i,k_{i+1}]$. This is a reasonable approach because $\xi_{n,k_\parallel}$ is known to be smooth

with respect to $k_\parallel$ on the bounded interval $[0,\kappa]$. Therefore we have to compute the matrices

$$\tilde{I}_{ij}^{(n)}(|z-z'|) = \int_0^{k_F^{(n)}} dk_\parallel' I(k_i,k_\parallel',|z-z'|)h_j(k_\parallel') = \int_{k_j}^{\min(k_{j+1},k_F^{(n)})} dk_\parallel' I(k_i,k_\parallel',|z-z'|) \quad \text{(A5)}$$

and

$$\bar{I}_{ij}^{(n,n')}(|z-z'|) = \int_0^{k_F^{(n)}} k_\parallel dk_\parallel \int_0^{k_F^{(n')}} dk_\parallel' I(k_\parallel,k_\parallel',|z-z'|)h_i(k_\parallel)h_j(k_\parallel') = \int_{k_i}^{\min(k_{i+1},k_F^{(n)})} k_\parallel dk_\parallel \int_{k_j}^{\min(k_{j+1},k_F^{(n')})} dk_\parallel' I(k_\parallel,k_\parallel',|z-z'|), \quad \text{(A6)}$$

for the Fock matrix and surface energy, respectively. Special care must be taken concerning the upper limits of the integrals, since the Fermi momenta $k_F^{(n)}$ are generally not located at a mesh point. Most of the entries of the matrices $\tilde{\mathbf{I}}^{(n)}$ and $\bar{\mathbf{I}}^{(n,n')}$ can be precomputed prior to the SCF iterations. Only those matrix elements which incorporate the Fermi surface have to be recomputed in each SCF cycle due to small changes in the Fermi momenta $k_F^{(n)}$. According to the decomposition (A1), we can separate the divergent part of the integrand and evaluate the corresponding integrals analytically, i.e., for $k_{i+1} \le k_F^{(n)}$ and $k_{j+1} \le k_F^{(n')}$:

$$\int_{k_j}^{k_{j+1}} dk_\parallel' I_1(k_\parallel,k_\parallel') = F(k_\parallel,k_{j+1}) - F(k_\parallel,k_j), \quad \text{(A7)}$$

with

$$F(k_\parallel,k_\parallel') = \frac{2}{3\pi\sqrt{k_\parallel}}(2(k_\parallel')^{3/2}\ln(\sqrt{k_\parallel}+\sqrt{k_\parallel'}) + ((k_\parallel)^{3/2} - (k_\parallel')^{3/2})\ln|k_\parallel - k_\parallel'| + k_\parallel'\sqrt{k_\parallel})$$

and

$$\int_{k_i}^{k_{i+1}} k_\parallel dk_\parallel \int_{k_j}^{k_{j+1}} dk_\parallel' I_1(k_\parallel,k_\parallel') = G(k_{i+1},k_{j+1}) - G(k_{i+1},k_j) - G(k_i,k_{j+1}) + G(k_i,k_j), \quad \text{(A8)}$$

with

$$G(k_\parallel,k_\parallel') = \frac{2}{9\pi}\{4(k_\parallel k_\parallel')^{3/2}\ln(\sqrt{k_\parallel}+\sqrt{k_\parallel'}) + [(k_\parallel)^{3/2} - (k_\parallel')^{3/2}]^2\ln|k_\parallel - k_\parallel'| + k_\parallel k_\parallel'(k_\parallel + k_\parallel')\}.$$

The remaining integrals with respect to I_0 can be efficiently determined numerically.

APPENDIX B: GALERKIN DISCRETIZATION AND ITERATIVE SOLUTION

In order to study the infinite slab, we first uniformly discretized the parallel momentum $k_\parallel$ on an interval $[0,\kappa]$ sufficiently large such that $k_F^{(n)} \le \kappa$. Subsequently, we have approximated the functions

$$\xi_{n,k_\parallel}(z) = \sum_a t_a^{n,k_\parallel}\phi_{j,a}(z) \quad \text{(B1)}$$

in an interpolating scaling function basis of Deslauriers and Dubuc.[58] The scaling function basis can be constructed from a mother function $\phi(z)$, shown in Fig. 9, via dilation and translation

$$\phi_{j,a}(z) = 2^{j/2}\phi(2^j z - a), \quad a = 0, \pm 1, \pm 2, \cdots, \quad \text{(B2)}$$

for a fixed resolution level j which has to be chosen large enough in order to keep the approximation error sufficiently small. For our calculations we have chosen a scaling function basis which provides an exact representation for polynomials up to fifth order. Thereby it is possible to keep the number of basis functions N_ϕ reasonably small, which is important because in each self-consistent iteration an eigenvalue problem has to be solved at every $k_\parallel$ point and the computational cost for such an operation scales as N_ϕ^3. In principle it would have been possible to switch to the corresponding biorthogonal compactly supported wavelet basis of Sweldens.[59] This enables an adaptive refinement near the slab surfaces and results in a further reduction of the size of the basis set. We refrained from this step in order to avoid further complications in the algorithm due to the hierarchical character of wavelet bases. We have chosen scaling functions at resolution level $j=0$ and $j=-1$, corresponding to grid distances of 1 and 2 bohrs, for the bulk electron densities $r_s=2$ and $r_s=4,6$, respectively. By choosing the next finer resolution level, the surface energy changes less than 1 erg/cm^2. Appropriate mesh sizes for the discretization of $k_\parallel$ and z keep the discretization error within a few erg/cm^2 for the surface energy.

Performing a Galerkin discretization of the HF equations in the scaling function basis we obtain

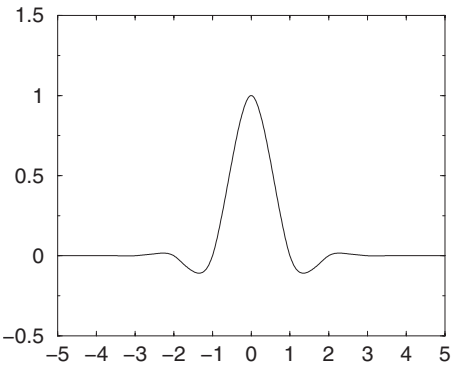

FIG. 9. Interpolating mother scaling function $\phi(z)$.

$$\sum_b (h_{ab} + J_{ab} + K_{ab}^{k_\parallel}) t_b^{n,k_\parallel} = \left(\epsilon_{n,k_\parallel} - \frac{1}{2} k_\parallel^2 \right) \sum_b S_{ab} t_b^{n,k_\parallel}, \quad \text{(B3)}$$

where the matrix elements are given by

$$h_{ab} = \frac{1}{2} \int_{-\infty}^{\infty} dz \frac{d}{dz} \phi_{j,a}^* \frac{d}{dz} \phi_{j,b}, \quad \text{(B4)}$$

$$J_{ab} = -2\pi \int_{-\infty}^{\infty} dz' \int_{-\infty}^{\infty} dz [\rho(z') - \rho_+(z')] |z - z'| \phi_{j,a}^*(z) \phi_{j,b}(z), \quad \text{(B5)}$$

$$K_{ab}^{k_\parallel} = -\sum_{n'} \int_{k_\parallel' \le k_F^{(n')}} dk_\parallel' \int_{-\infty}^{\infty} dz' \int_{-\infty}^{\infty} dz \phi_{j,a}^*(z) \phi_{j,b}(z') \xi_{n',k_\parallel'}^*(z') \times \xi_{n',k_\parallel'}(z) I(k_\parallel, k_\parallel', |z - z'|), \quad \text{(B6)}$$

$$S_{ab} = \int_{-\infty}^{\infty} dz \phi_{j,a}^*(z) \phi_{j,b}(z). \quad \text{(B7)}$$

For the sake of notational simplicity, we suppressed the j dependence of the matrix elements. The ith self-consistent HF iteration comprises the following steps: (1) Determine the new Fermi energy $\epsilon_F^{(i)}$ and Fermi momenta $k_F^{(n)(i)}$ from the previous iteration; (2) calculate $J_{ab}^{(i)}$ from $\xi_{n,k_\parallel}^{(i-1)}$; (3) for all mesh points $k_\parallel$: calculate $K_{ab}^{k_\parallel(i)}$ and solve the eigenvalue problem to get $\epsilon_{n,k_\parallel}^{(i)}$ and $\xi_{n,k_\parallel}^{(i)}$; and (4) go to step 1 until self-consistency has been achieved.

TABLE II. Storage requirements of the basic quantities in a self-consistent HF calculation.

objects	$k_\parallel$	z	$\phi_\alpha(z)$	$\epsilon_{n,k_\parallel}$	$\xi_{n,k_\parallel}(z)$	$\rho(z)$	I_0	$\mathbf{h},\mathbf{S},\mathbf{J},\mathbf{K}$
storage	N_k	N_z	$N_\phi N_z$	$N_n N_k$	$N_n N_k N_z$	N_z	$N_k^2 N_z$	N_ϕ^2

The calculation of the integrals (B5) and (B6) has to be performed numerically. We have used the approximation (A4) together with Eq. (A5) in order to compute the integrals over $k_\parallel$. For the remaining integrals over z, z', we transformed the scaling functions $\phi_{j,a}$ on a sufficiently fine level $l \gg j$ using the refinement relation

$$\phi(x) = 2 \sum_a h_a \phi(2x - a), \quad \text{(B8)}$$

involving only a finite number of filter coefficients h_a. Using the interpolation property of the scaling functions, we simply represented the integrands of Eq. (B5) and (B6) on regular two-dimensional grids of size N_z^2 and grid spacing 2^{-l} bohrs. Combining neighboring grid points, we finally compute the integrals in a straightforward manner according to Simpson's rule. The storage requirements of our basic quantities are listed in Table II, where N_n denotes the total number of size-quantized levels and N_k refers to the number of mesh points required for the discretization of $k_\parallel$. As expected, the CPU time dominating step turned out to be the calculation of the exchange matrix (B6) which scales as $N_n^2 N_k^2 N_\phi^2 N_z^2$.

*Present address: Institut für Mathematik, Technische Universität Berlin, Straße des 17. Juni 136, D-10623 Berlin, Germany.

[1] T. Ando, A. B. Fowler, and F. Stern, Rev. Mod. Phys. **54**, 437 (1982).
[2] S. L. Chuang, *Physics of Optoelectronic Devices* (Wiley, New York, 1995).
[3] S. Goedecker and I. Ivanov, Solid State Commun. **105**, 665 (1998).
[4] T. A. Arias, Rev. Mod. Phys. **71**, 267 (1999).
[5] T. D. Engeness and T. A. Arias, Phys. Rev. B **65**, 165106 (2002).
[6] K. S. Thygesen, M. V. Bollinger, and K. W. Jacobsen, Phys. Rev. B **67**, 115404 (2003).
[7] A. I. Neelov and S. Goedecker, J. Comput. Phys. **217**, 312 (2006).
[8] L. Genovese, T. Deutsch, A. Neelov, S. Goedecker, and G. Beylkin, J. Chem. Phys. **125**, 074105 (2006).
[9] L. Genovese, T. Deutsch, and S. Goedecker, J. Chem. Phys. **127**, 054704 (2007).
[10] H.-J. Flad, W. Hackbusch, H. Luo, and D. Kolb, J. Comput. Phys. **205**, 540 (2005).
[11] H.-J. Flad, W. Hackbusch, H. Luo, and D. Kolb, Phys. Rev. B **71**, 125115 (2005).
[12] H. Luo, D. Kolb, H.-J. Flad, and W. Hackbusch, Phys. Rev. B **75**, 125111 (2007).
[13] M. Nekovee and J. M. Pitarke, Comput. Phys. Commun. **137**, 123 (2001).
[14] N. D. Lang and W. Kohn, Phys. Rev. B **1**, 4555 (1970).
[15] N. D. Lang and W. Kohn, Phys. Rev. B **3**, 1215 (1971).
[16] J. Harris and R. O. Jones, J. Phys. F: Met. Phys. **4**, 1170 (1974).
[17] D. C. Langreth and J. P. Perdew, Solid State Commun. **17**, 1425 (1975).
[18] J. P. Perdew, D. C. Langreth, and V. Sahni, Phys. Rev. Lett. **38**, 1030 (1977).
[19] V. Sahni and J. Gruenebaum, Phys. Rev. B **19**, 1840 (1979).
[20] V. Sahni, J. Gruenebaum, and J. P. Perdew, Phys. Rev. B **26**, 4371 (1982).
[21] Z. Y. Zhang, D. C. Langreth, and J. P. Perdew, Phys. Rev. B **41**, 5674 (1990).
[22] J. M. Pitarke and A. G. Eguiluz, Phys. Rev. B **57**, 6329 (1998).
[23] S. Kurth and J. P. Perdew, Phys. Rev. B **59**, 10461 (1999).
[24] J. M. Pitarke and A. G. Eguiluz, Phys. Rev. B **63**, 045116 (2001).
[25] A. E. Mattsson and W. Kohn, J. Chem. Phys. **115**, 3441 (2001).
[26] J. F. Dobson, J. Wang, and T. Gould, Phys. Rev. B **66**, 081108(R) (2002).
[27] J. M. Pitarke and J. P. Perdew, Phys. Rev. B **67**, 045101 (2003).
[28] J. F. Dobson and J. Wang, Phys. Rev. B **69**, 235104 (2004).
[29] X. Sun, T. Li, M. Farjam, and C. W. Woo, Phys. Rev. B **27**, 3913

(1983).
[30] X. Sun, M. Farjam, and C. W. Woo, Phys. Rev. B **28**, 5599 (1983).
[31] E. Krotscheck, W. Kohn, and G.-X. Qian, Phys. Rev. B **32**, 5693 (1985).
[32] E. Krotscheck and W. Kohn, Phys. Rev. Lett. **57**, 862 (1986).
[33] X.-P. Li, R. J. Needs, R. M. Martin, and D. M. Ceperley, Phys. Rev. B **45**, 6124 (1992).
[34] P. H. Acioli and D. M. Ceperley, Phys. Rev. B **54**, 17199 (1996).
[35] Z. Yan, J. P. Perdew, S. Kurth, C. Fiolhais, and L. Almeida, Phys. Rev. B **61**, 2595 (2000); **64**, 049904(E) (2001).
[36] J. M. Pitarke, Phys. Rev. B **70**, 087401 (2004).
[37] J. Bardeen, Phys. Rev. **49**, 653 (1936).
[38] C. Q. Ma and V. Sahni, Phys. Rev. B **20**, 2291 (1979).
[39] V. Sahni and C. Q. Ma, Phys. Rev. B **22**, 5987 (1980).
[40] V. Sahni and K.-P. Bohnen, Phys. Rev. B **29**, 1045 (1984).
[41] V. Sahni and K.-P. Bohnen, Phys. Rev. B **31**, 7651 (1985).
[42] M. K. Harbola and V. Sahni, Phys. Rev. B **37**, 745 (1988).
[43] V. Sahni, Surf. Sci. **213**, 226 (1989).
[44] V. Sahni and J. Gruenebaum, Solid State Commun. **21**, 463 (1977).
[45] V. Sahni, J. B. Krieger, and J. Gruenebaum, Phys. Rev. B **15**, 1941 (1977).
[46] V. Sahni, C. Q. Ma, and J. S. Flamholz, Phys. Rev. B **18**, 3931 (1978).
[47] V. Sahni, *Quantal Density Functional Theory* (Springer, Berlin, 2004).
[48] P. Fulde, *Electron Correlations in Molecules and Solids*, 3rd ed. (Springer, Berlin, 1995).
[49] A. Szabo and N. S. Ostlund, *Modern Quantum Chemistry* (McGraw-Hill, New York, 1989).
[50] F. Mertins, Ann. Phys. **8**, 261 (1999).
[51] F. K. Schulte, Surf. Sci. **55**, 427 (1976).
[52] J. P. Rogers III, P. H. Cutler, T. E. Feuchtwang, and A. A. Lucas, Surf. Sci. **181**, 436 (1987).
[53] F. K. Schulte, J. Phys. C **7**, L370 (1974).
[54] R. Monnier, J. P. Perdew, D. C. Langreth, and J. W. Wilkins, Phys. Rev. B **18**, 656 (1978).
[55] J. P. Perdew and V. Sahni, Solid State Commun. **30**, 87 (1979).
[56] E. P. Wigner, Phys. Rev. **46**, 1002 (1934).
[57] H. J. Monkhorst, Phys. Rev. B **20**, 1504 (1979).
[58] G. Deslauriers and S. Dubuc, Constructive Approx. **5**, 49 (1989).
[59] W. Sweldens, Appl. Comput. Harmon. Anal. **3**, 186 (1996).